

Silibinin Targeting Heat Shock Protein 90 Represents a Novel Approach to Alleviate Nonalcoholic Fatty Liver Disease by Simultaneously Lowering Hepatic Lipotoxicity and Enhancing Gut Barrier Function

Baofei Yan,[#] Xian Zheng,[#] Xi Chen, Huihui Hao, Shen Shen, Jingwen Yang, Siting Wang, Yuping Sun, Jiaqi Xian, Zhitao Shao, and Tingming Fu*



Cite This: <https://doi.org/10.1021/acspsci.4c00185>



Read Online

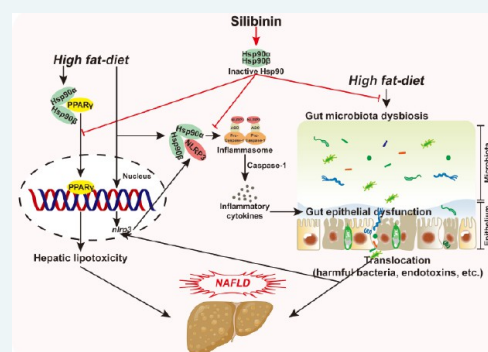
ACCESS |

Metrics & More

Article Recommendations

ABSTRACT: Nonalcoholic fatty liver disease (NAFLD) is a clinicopathological condition characterized by intrahepatic ectopic steatosis. Due to the increase in high-calorie diets and sedentary lifestyles, NAFLD has surpassed viral hepatitis and become the most prevalent chronic liver disease globally. Silibinin, a natural compound, has shown promising therapeutic potential for the treatment of liver diseases. Nevertheless, the ameliorative effects of silibinin on NAFLD have not been completely understood, and the underlying mechanism is elusive. Therefore, in this study, we used high-fat diet (HFD)-induced mice and free fatty acid (FFA)-stimulated HepG2 cells to investigate the efficacy of silibinin for the treatment of NAFLD and elucidate the underlying mechanisms. *In vivo*, silibinin showed significant efficacy in inhibiting adiposity, improving lipid profile levels, ameliorating hepatic histological aberrations, healing the intestinal epithelium, and restoring gut microbiota compositions. Furthermore, *in vitro*, silibinin effectively inhibited FFA-induced lipid accumulation in HepG2 cells. Mechanistically, we reveal that silibinin possesses the ability to ameliorate hepatic lipotoxicity by suppressing the heat shock protein 90 (Hsp90)/peroxisome proliferator-activated receptor- γ (PPAR γ) pathway and alleviating gut dysfunction by inhibiting the Hsp90/NOD-like receptor pyrin domain-containing 3 (NLRP3) pathway. Altogether, our findings provide evidence that silibinin is a promising candidate for alleviating the “multiple-hit” in the progression of NAFLD.

KEYWORDS: NAFLD, silibinin, hepatic lipotoxicity, Hsp90/PPAR γ pathway, Hsp90/NLRP3 pathway, gut barrier function



1. INTRODUCTION

Nonalcoholic fatty liver disease (NAFLD) is a clinicopathological condition characterized by the excessive accumulation of fat in the liver (more than 5% of liver weight), which is not related to alcohol consumption or other liver-damaging factors, including medications, viral infections, or autoimmune disorders.¹ The prevalence of NAFLD has increased considerably due to the rise in obesity among the population. NAFLD affects approximately 3–18% of adolescents, 25–30% of the general population, and 70–90% of individuals with obesity or diabetes globally.¹ NAFLD includes a spectrum of liver conditions, such as nonalcoholic fatty liver (NAFL) and nonalcoholic steatohepatitis (NASH). If left untreated, NAFLD can progress to liver fibrosis, cirrhosis, or even hepatocellular carcinoma.² Furthermore, NAFLD is linked with an increased risk of type II diabetes, cardiovascular disease (CVD), heart disease, and chronic kidney disease, further increasing the mortality rate due to CVD by 64%.³ Nevertheless, presently only one drug, namely resmetirom, has been

approved by the U.S. FDA for the treatment of NASH, while its benefits still need to be supported by long-term and large-scale clinical evidence. Proverbially recommended approaches for managing NAFLD, such as lifestyle alterations including calorie restriction and increased physical activity, are usually not regularly followed by patients.⁴ NAFLD has emerged as a considerable global public health concern due to its high prevalence, the large number of affected individuals, and its potential severity. Therefore, safe and effective therapeutic drugs for the treatment of NAFLD are urgently required.

Received: April 1, 2024

Revised: June 11, 2024

Accepted: June 14, 2024

NAFLD is a multifactorial disorder with a complex pathogenesis. The “multiple-hit” hypothesis indicates that NAFLD stems from hepatic lipotoxicity due to dysregulated lipid metabolism, causing oxidative stress, inflammation, and compromised gut barrier, which further contributes to its progression.^{5,6} The suppression of lipogenesis and promotion of lipolysis are potential therapeutic strategies for the treatment of NAFLD. Furthermore, peroxisome proliferator-activated receptor- γ (PPAR γ) has emerged as a major regulator of lipid metabolism and insulin sensitivity.⁷ In mouse models, the hepatic expression of PPAR γ is upregulated in steatosis due to obesity, and the modulation of PPAR γ is important for managing steatosis.^{7,8} For instance, PPAR γ activation can trigger *de novo* lipogenesis, increase triglyceride (TG) accumulation, and induce insulin sensitivity and lipotoxicity.⁹ Heat shock protein 90 (Hsp90) is a molecular chaperone involved in PPAR γ regulation, and inhibitors of Hsp90 can block PPAR γ activity.^{10,11} Furthermore, NAFLD is also characterized by gut dysbiosis and increased permeability, where the activation of the NOD-like receptor pyrin domain-containing 3 (NLRP3) inflammasome and gut inflammation plays a crucial role.^{12–14} Hsp90/NLRP3 interaction plays an important role in NAFLD progression. Hence, Hsp90 inhibition can be a potential strategy to inhibit NLRP3 inflammasome activity.^{15,16} Therefore, targeting Hsp90 can be a novel strategy for NAFLD treatment, restoring hepatic metabolic dysregulation and gut barrier dysfunction.

Silybum marianum (*S. marianum*), also known as milk thistle, is an herbaceous plant belonging to the Asteraceae family.¹⁷ The dried mature fruits of *S. marianum* have been widely used in traditional medicines in European and East Asian countries as a dietary additive or hepatoprotective agent.¹⁷ Silibinin, a bioactive component of *S. marianum*, has been widely used for the treatment and experimental studies of liver disorders, such as NAFLD, showing favorable outcomes.^{18,19} Nevertheless, the efficacy of silibinin for treating NAFLD lacks evidence, and its underlying mechanisms are not completely elucidated. Silibinin is a potent C-terminal Hsp90 inhibitor, with promising potential in treating Hsp90-associated diseases.²⁰ Researchers have found that silibinin can considerably ameliorate the effects of high-fat diet (HFD)-induced NASH in mice. The effect of silibinin is mediated by inhibiting PPAR γ activity, indicating that silibinin can suppress the Hsp90/PPAR γ pathway during the progression of NAFLD.²¹ Moreover, following its oral administration, the unabsorbed part of silibinin can affect the gut microbiota and its secondary metabolites, including short-chain fatty acids (SCFAs) and bile acids.²² Silibinin can decrease the production of inflammatory cytokines and maintain the integrity of the intestinal epithelium, which is closely associated with inhibiting the Hsp90/NLRP3 pathway in guts.²³ These changes indirectly contribute to the inhibition of NAFLD progression through the gut–liver axis. Therefore, the gut is considered an important target of silibinin. Based on these findings, we hypothesize that silibinin may play a therapeutic role in NAFLD based on the intrahepatic and extrahepatic aspects. Silibinin can suppress the Hsp90/PPAR γ pathway in livers and the Hsp90/NLRP3 pathway in guts, thereby improving microbiota dysbiosis. In this study, we established a mouse model of HFD-induced NAFLD and free fatty acid (FFA)-stimulated HepG2 cells to investigate the inhibitory effects of silibinin. We aimed to elucidate the mechanism underlying

silibinin, with a particular focus on the hepatic Hsp90–PPAR γ and the gut-associated Hsp90/NLRP3 pathways.

2. MATERIALS AND METHODS

2.1. Chemicals and Reagents. Silibinin (Sil) with a purity of $\geq 98\%$ was laboratory made, which showed silibinin A and silibinin B in a molar ratio of 1:1. Asiatic acid with a purity of $\geq 99\%$ was purchased from MCE company (New Jersey, USA).²⁴ Kits for hematoxylin and eosin stain (H&E), Oil Red O, periodic acid-schiff (PAS), interleukin-6 (IL-6), interleukin- 1β (IL- 1β), and tumor necrosis factor- α (TNF- α) were provided by Servicebio Biotechnology (Wuhan, China). Commercial biochemical kits for measuring TG, total cholesterol (TC), low-density lipoprotein cholesterol (LDL-c), high-density lipoprotein cholesterol (HDL-c), alanine aminotransferase (ALT), and aspartate aminotransferase (AST) were obtained from Nanjing Jiancheng Bioengineering Institute (Nanjing, China). Dulbecco’s modified Eagle medium (DMEM), fetal bovine serum (FBS), bovine serum albumin (BSA), sodium oleate, and sodium palmitate were purchased from Sigma-Aldrich (St Louis, MO, USA). Penicillin–Streptomycin solution was procured from Thermo Fisher Scientific (Waltham, MA, USA). Fatty acid-free BSA was procured from Solarbio Biotechnology (Beijing, China). Antibodies against Hsp90 α , Hsp90 β , apoptosis-associated speck-like protein containing a CARD (ASC), and β -actin were provided by Abcam (Cambridge, UK); the antibody against PPAR γ was provided by Cell Signaling Technology (Boston, USA); antibodies against mucin 2 (MUC2), zonula occludens-1 (ZO-1), and occludin were provided by Affinity Biosciences (Changzhou, China); and antibodies against NLRP3 and caspase-1 were provided by MedChemExpress (New Jersey, USA). All other chemicals were of analytical grade.

2.2. Animals. Male C57BL/6 mice, 6 weeks old and weighing 20–24 g, were procured from Gempharmatech Co., Ltd. (Nanjing, China). The mice were kept under standard laboratory conditions at the Jiangsu Health Vocational College Laboratory Animal Center, with a humidity of 40–50%, a temperature of 25 ± 1 °C, a 12 h light/dark cycle, and *ad libitum* access to food and water. All experimental procedures were performed in accordance with the European Community guidelines. The study obtained approval from the Animal Ethics Committee of Jiangsu Health Vocational College (Approval No. JHVC-IACUC-2022-B007).

2.3. Animal Grouping and Treatment. After a seven-day acclimatization period, mice were randomly assigned to four groups ($n = 6$ /group): normal chow diet (NCD), high-fat diet (HFD), HFD with asiatic acid (100 mg/kg), and HFD with silibinin (100 mg/kg). The dose of silibinin was selected referring to its clinical dosage and previous studies.²⁵ The NCD group was provided a standard chow diet with 10% of calories derived from fat, whereas the other groups were subjected to an HFD constituting 60% of calories from fat to induce NAFLD for 16 weeks. Starting from the fourth week, mice in the intervention groups were orally administered the respective drugs once daily. Mice in the NCD and HFD groups were administered with an equivalent volume of 0.5% CMC-Na orally as a control.

2.4. Cell Culture and Treatment. As previously mentioned, a specific combination of sodium oleate and sodium palmitate, forming FFA, was utilized to induce intracellular fat accumulation.²⁶ HepG2 cells, procured from

Table 1. Primers Used in This Study

gene	primers (5'→3')	
	forward	reverse
<i>M-Hsp90aa1</i>	TGAGGAAACCCAGACCCAAGA	GCTGGGAATGAGATTGATGTGC
<i>M-Hsp90ab1</i>	AAGGAGTTTGATGGGAAGAGCC	GGAGATTGTCACCTTTTCAACCTTC
<i>M-Pparγ</i>	GACCACTCGCATTCTTTGACA	ATCGCACTTTGGTATTCTTGGA
<i>M-β-actin</i>	GTGACGTTGACATCCGTAAAGA	GTAACAGTCCGCCTAGAAGCAC

the Chinese Academy of Cell Resource Center (Shanghai, China), were cultured in DMEM supplemented with 10% FBS and 1% penicillin–streptomycin at 37 °C in a humidified 5% CO₂ environment. For experimental interventions, HepG2 cells in a serum-free medium at approximately 70% confluency for 12 h were subjected to treatment with either asiatic acid (20 μM) or silibinin (20 μM) in the presence of 1 mM FFA for 24 h. HepG2 cells grown in serum-free medium supplemented with 5% BSA served as the blank control. The overexpression plasmids for Hsp90α and Hsp90β were obtained from Vigene Bioscience, Inc. (Jinan, China), and their transfection was performed using Lipofectamine 3000 (Invitrogen, Carlsbad, CA, USA) following the manufacturer's protocols. Subsequently, the cells were either harvested for Western blotting or treated with silibinin (20 μM).

2.5. Assessment of NAFLD. Weekly monitoring of body weight and food intake was performed throughout the experimental period. At the conclusion of the study, mice underwent an overnight fast and were subsequently anesthetized with 10% pentobarbital sodium and sacrificed by CO₂ inhalation. Tissues of interest were quickly excised and rinsed using PBS. Liver weights were recorded for the calculation of the liver index (liver weight/body weight ratio). Serum samples, tissue homogenates, and HepG2 cell supernatants were obtained using standard protocols. Various parameters, such as TG, TC, LDL-c, HDL-c, ALT, AST, IL-6, IL-1β, and TNF-α, were evaluated in these samples. Fixed liver and colon tissues were embedded in paraffin, sectioned into 5 μm slices, and used for pathological staining, including H&E, Oil Red O, and PAS. Similarly, fixed HepG2 cells were also stained with Oil Red O dye.

2.6. Immunohistochemical/Immunofluorescent Analysis. Consistent with our previous methodology,²⁷ immunohistochemical and immunofluorescent evaluations were performed on the aforementioned sections. Primary antibodies targeting Hsp90α, Hsp90β, PPARγ, MUC2, ZO-1, occludin, NLRP3, ASC, and caspase-1 were diluted 200-fold and incubated with the slices overnight at 4 °C. Furthermore, 100 μL of secondary antibody, diluted 400-fold, was added dropwise to each section. For the detection of Hsp90α, Hsp90β, PPARγ, MUC2, ZO-1, occludin, NLRP3, ASC, and caspase-1, HRP-conjugated goat antirabbit IgG (H+L) and DAB were used. Furthermore, Alexa Fluor594-conjugated goat antirabbit IgG (H+L), DAPI, and DAB were sequentially applied for Hsp90α, Hsp90β, and PPARγ detection. The images were obtained using either a Zeiss LSM 700 confocal laser microscope (Oberkochen, Germany) or a Leica DM2500 optical microscope (Wetzlar, Germany). Last, Image-Pro Plus 6.0 software was used for data analysis (Media Cybernetics, Maryland, USA).

2.7. RNA-Seq Analysis of Liver. Total RNA from the liver tissues was extracted and evaluated for quality and concentration using a NanoRhatometer@spectrophotometer (IM-PLLEN, CA, USA) and an Agilent Bioanalyzer 2100 system,

respectively. The sequencing library was established using an RNA Library Prep kit, and sequencing was conducted on the Illumina Novaseq 6000 system (San Diego, CA, USA). The raw data obtained underwent processing, filtering, and sequencing analysis using the Majorbio Cloud online platform (www.majorbio.com), following a previously described method.²⁵

2.8. Real-Time Polymerase Chain Reaction (RT-PCR). Liver tissues and HepG2 cells underwent total RNA extraction using an RNA extraction kit (Servicebio) and were quantified using the Nanodrop 2000 spectrophotometer (Thermo Fisher Scientific) according to standard protocols. Subsequently, a reverse transcription reaction system (Servicebio) was used to process the RNA samples. Quantitative RT-PCR was performed using an RT-PCR system (Biorad, CA, USA), following the methodology described in our previous investigation.²⁶ The primer sequences were designed by Servicebio (Table 1). The expression of the target genes was quantified using the 2^{-ΔΔCt} method, and β-actin was used as the control for normalization.

2.9. Western Blotting. Prechilled RIPA buffer containing a protease inhibitor cocktail was used for the lysis of collected cells and liver tissues. The total protein content was quantified using a commercially available BCA assay kit. Immunoblot analysis was performed according to the established protocols.²⁷ Primary antibodies against Hsp90α, Hsp90β, PPARγ, MUC2, ZO-1, occludin, NLRP3, ASC, caspase-1, and β-actin were used at a dilution of 1:1000. The Azure Biosystems C600 (Azure Biosystems Inc., CA, USA) and ImageJ software (NIH, Bethesda, MD, USA) were used for visualization and semiquantification of the bands, respectively.

2.10. 16S rRNA Sequencing. Following standard procedures, the bacterial genome present in the colonic contents was extracted using the E.Z.N.A. soil DNA kit (Omega Bio-Tek, GA, USA) and identified using the spectrophotometer mentioned earlier. PCR was performed using previously described primers.²⁸ Then, the MiSeq platform (Illumina, San Diego, USA) was used for sequencing and pair-end analysis. The resulting raw fastq file was processed and analyzed using the Majorbio Cloud online platform (www.majorbio.com) using our previously described method.²⁹

2.11. Statistical Analysis. IBM SPSS 21.0 software (Armonk, USA) was used for data analysis. Data are presented as the mean ± standard deviation (SD). Statistical significance among groups was determined by performing one-way ANOVA followed by Tukey's posthoc test for multiple comparisons. A *p*-value of <0.05 was considered statistically significant.

3. RESULTS

3.1. Silibinin Alleviated Adiposity and Hepatic Abnormalities in HFD-Induced NAFLD Mice. Excessive consumption of HFD has become a feature of a modern

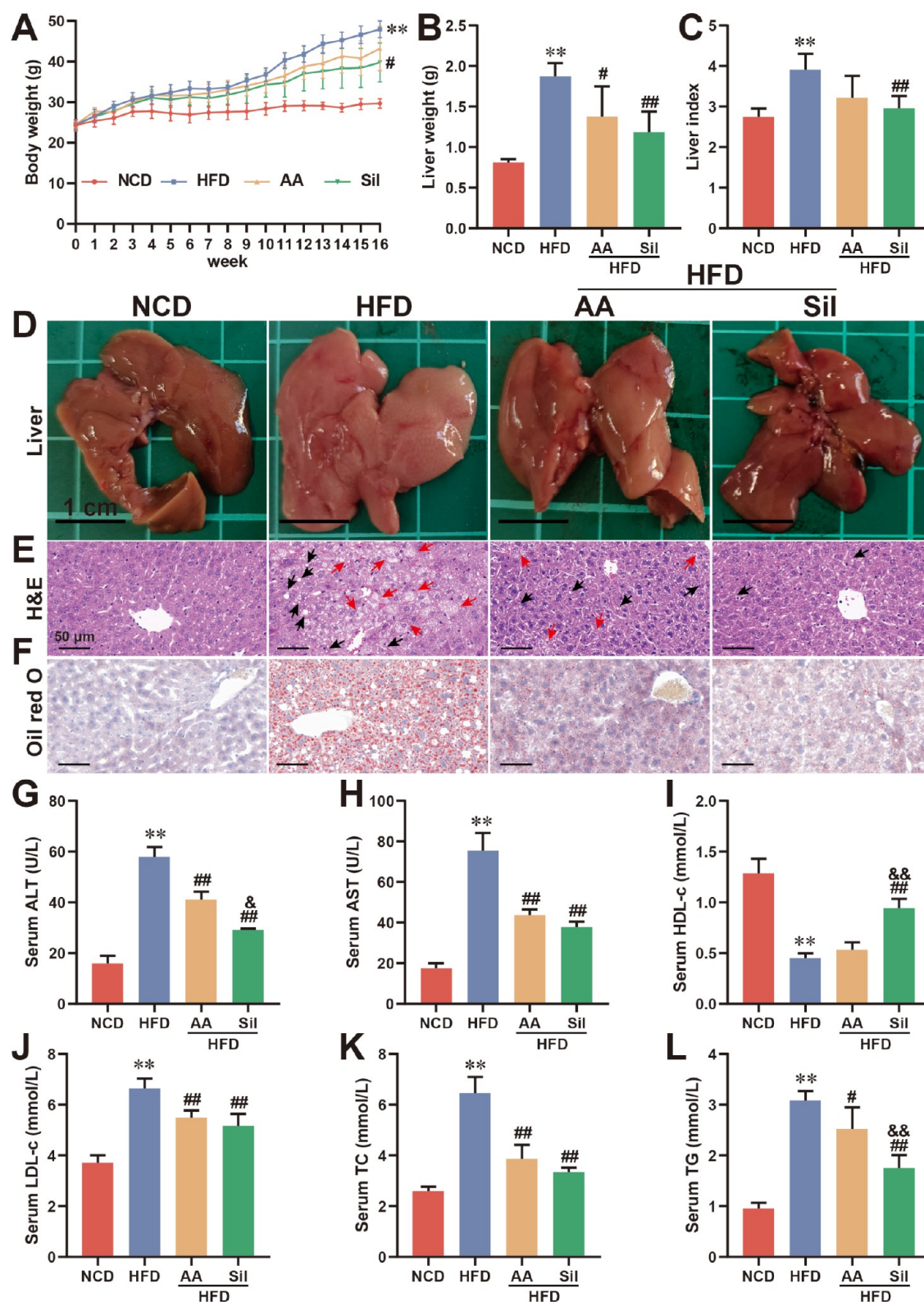


Figure 1. Silibinin improved body weight, hepatic steatosis, lipid disorders, and liver injuries in HFD-fed mice. (A) Dynamic curve of the body weight, (B) liver weight, and (C) liver index of mice. (D) Phenotypic presentation of livers. Representative micrographs of H&E (E) and Oil Red O (F) stainings. (G–L) The serum levels of ALT, AST, HDL-c, LDL-c, TC, and TG. Data are presented as the mean \pm SD ($n = 5$). $**p < 0.01$ vs the NCD group, $\#p < 0.05$ and $\#\#p < 0.01$ vs the HFD group, and $\&p < 0.05$ and $\&\&p < 0.01$ vs the AA group. Sil, silibinin; AA, asiatic acid.

lifestyle and is primarily responsible for NAFLD emergence.³⁰ In this study, asiatic acid was chosen as a positive control owing to its impressive therapeutic potency on metabolic

syndromes, as revealed in our pilot experiments.^{31–33} Figure 1A–C illustrates that under model conditions, body and liver weights and liver index significantly decreased in response to

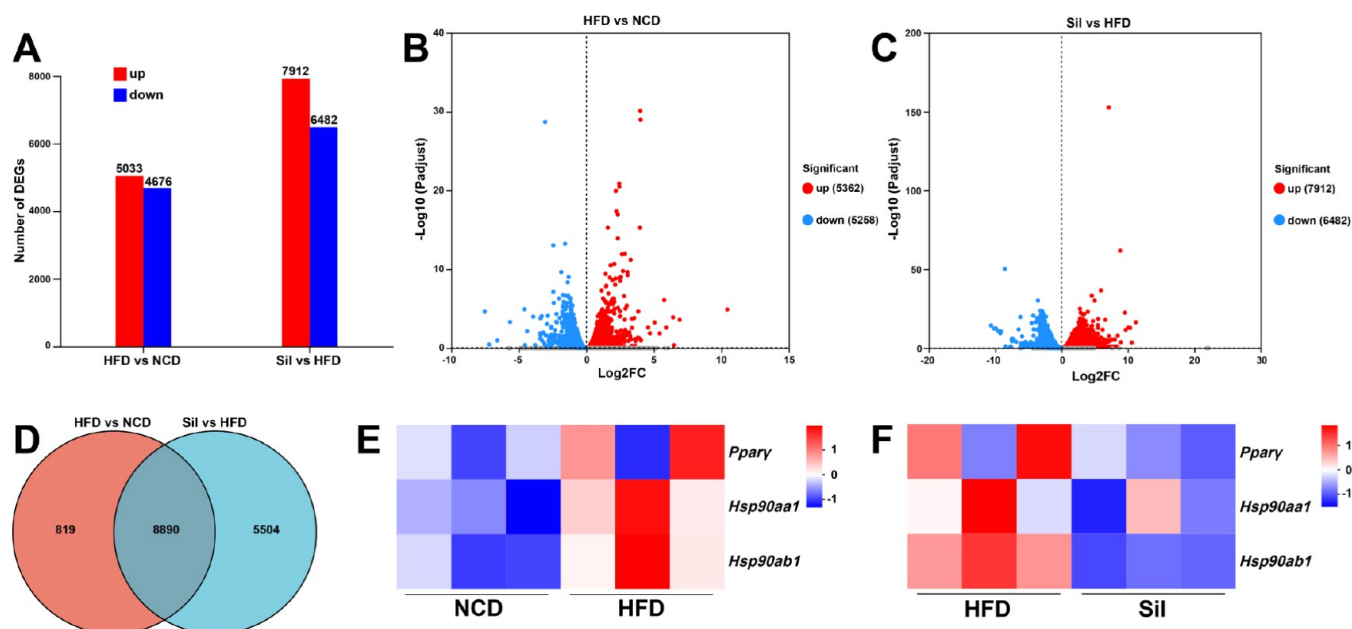


Figure 2. Silibinin regulated liver gene expression profile in HFD-fed mice. (A) The numbers of up- and downregulated DEGs among groups. Volcanic plot of different genes in expression of HFD vs NCD (B) and Sil vs HFD (C). (D) Venn diagram of the DEGs among groups. (E–F) The expression profile of *Hsp90aa1*, *Hsp90ab1*, and *Pparγ* among groups shown as heatmaps. Sil, silibinin.

silibinin administration. Because individuals with NAFLD frequently exhibit pathological abnormalities in their livers, histological analysis was conducted to determine the effects of silibinin. Macroscopically, the livers of mice in the HFD group were enlarged, had blurred borders, and exhibited severe steatosis; however, oral administration of silibinin improved these pathological changes (Figure 1D). H&E staining revealed severe destruction of the liver's lobular structure, steatosis, and hepatocellular ballooning degeneration in the mice in the HFD group. However, silibinin treatment mitigated these pathological alterations, as evidenced by the relatively intact liver lobules and smaller fat vacuoles (Figure 1E). Oil Red O staining revealed the conspicuous presence of lipid droplets in the HFD group; these droplets markedly decreased after silibinin treatment (Figure 1F).

In clinical settings, biochemical markers such as liver injury-related ALT and AST and lipid metabolism-related HDL-c, LDL-c, TC, and TG are used to diagnose NAFLD.²⁸ Compared with the NCD group, serum ALT, AST, LDL-c, TC, and TG levels were significantly increased in the HFD group; however, they were significantly decreased after silibinin treatment (Figure 1G–L). On the other hand, HDL-c levels were lower in the HFD group than in the NCD group; however, these levels rapidly recovered after silibinin treatment. Collectively, these findings suggest that silibinin effectively ameliorates HFD-induced obesity, hepatic steatosis, lipid abnormalities, and liver injury. Notably, at equivalent doses, silibinin demonstrated higher efficacy compared with asiatic acid.

3.2. Silibinin Targeted the Hsp90–PPAR γ Pathway in HFD-Induced NAFLD Mice. We conducted hepatic transcriptome sequencing to elucidate the potential molecular mechanism underlying the therapeutic effects of silibinin in NAFLD. Differential expression analysis of the HFD and NCD groups revealed 5033 upregulated differentially expressed genes (DEGs) and 4676 downregulated DEGs. Furthermore, compared with the HFD group, 7912 genes were upregulated

and 6482 genes were downregulated in the silibinin group. The Venn diagram in Figure 2D reveals 8890 shared DEGs among all groups, including *Hsp90aa1* (encoding Hsp90 α), *Hsp90ab1* (encoding Hsp90 β), and *Pparγ* (encoding PPAR γ). Notably, the mRNA expression of *Hsp90aa1*, *Hsp90ab1*, and *Pparγ* considerably increased in the HFD group (Figure 2E). Oral administration of silibinin appropriately restored most gene expression changes (Figure 2F). These results suggest that silibinin exerts its effects on NAFLD by inhibiting the Hsp90/PPAR γ pathway.

Next, we further validated the regulatory actions of silibinin on the genes and proteins associated with the Hsp90/PPAR γ pathway. Figure 3A–C illustrates that compared with the NCD group, *Hsp90aa1*, *Hsp90ab1*, and *Pparγ* were significantly upregulated in the HFD group. However, oral administration of silibinin effectively reversed these changes. Moreover, protein expression analysis revealed that Hsp90 α , Hsp90 β , and PPAR γ levels were markedly increased in the HFD group but were significantly decreased in the silibinin group (Figure 3D–G). These findings were consistent with the immunostaining results (Figure 3H–Q), where the immunostaining intensities (brown/fluorescence) of Hsp90 α , Hsp90 β , and PPAR γ were high in the HFD group, indicating the upregulation and activation of the Hsp90/PPAR γ pathway. However, silibinin administration substantially alleviated the changes observed in the immunohistochemical analysis. In summary, our findings highlight the significant association between the therapeutic effects of silibinin and the modulation of the Hsp90/PPAR γ pathway in alleviating NAFLD.

3.3. Silibinin Inhibited Fat Accumulation in FFA-Induced HepG2 Cells via the Hsp90–PPAR γ Pathway. In general, NAFLD symptoms are stimulated *in vitro* by exposing HepG2 cells to FFA.³⁰ Therefore, we used FFA-induced HepG2 cells to further elucidate the hepatoprotective properties and associated mechanisms of silibinin in NAFLD. Our preliminary results indicated that when coincubated with FFA (1 mM) at doses $\leq 100 \mu\text{M}$, neither silibinin nor asiatic acid

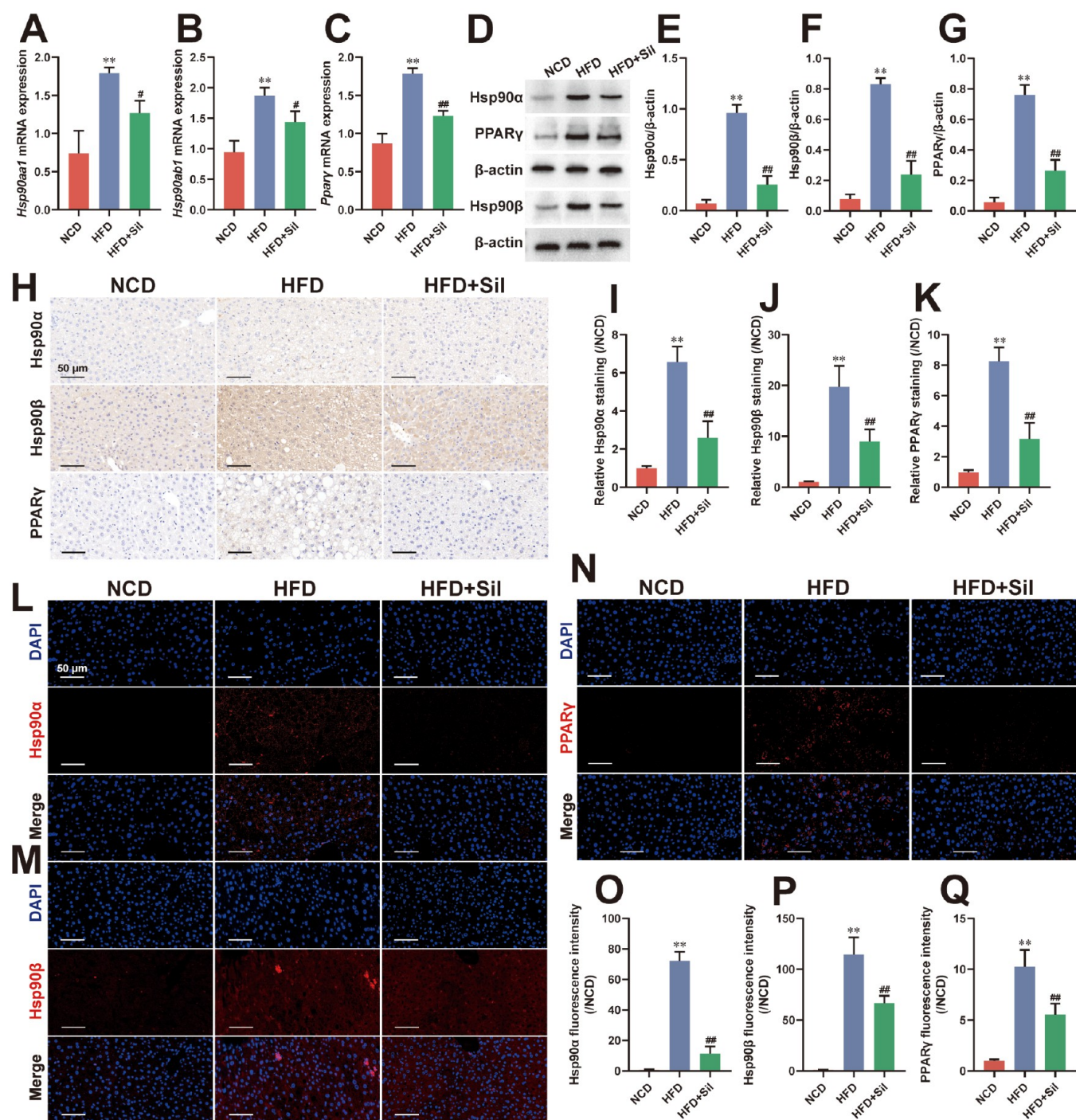


Figure 3. Silibinin inhibited the Hsp90/PPAR γ pathway in HFD-fed mice. (A–C) The mRNA expression of *Hsp90a1*, *Hsp90ab1*, and *Ppar γ* . (D) The expressions and (E–G) semiquantitative analysis of Hsp90 α , Hsp90 β , and PPAR γ . (H) Representative immunohistochemical images and (I–K) quantitative analysis of the staining intensity of Hsp90 α , Hsp90 β , and PPAR γ in the liver sections. (L–M) Representative fluorescent images and (O–Q) quantitative analysis of the fluorescence intensity of Hsp90 α , Hsp90 β , and PPAR γ in the liver sections. Data are presented as the mean \pm SD ($n = 3$). ** $p < 0.01$ vs the NCD group and # $p < 0.05$ and ## $p < 0.01$ vs the HFD group. Sil, silibinin.

exhibited noticeable cytotoxic effects on HepG2 cells. Therefore, 20 μ M silibinin and asiatic acid were selected to treat FFA-induced HepG2 cells for subsequent experiments. Oil Red O staining revealed the presence of a large number of lipid droplets in the FFA-induced group; in contrast, this pathological phenomenon was remarkably attenuated in the silibinin group, which is supported by an evident decrease in the number of lipid droplets (Figure 4A). Consistently, as demonstrated in Figure 4B,C, the levels of neutral lipids such

as TC and TG were significantly increased in FFA-induced HepG2 cells compared with those in control cells; the levels markedly decreased after silibinin treatment. Notably, in this context, the therapeutic effectiveness of silibinin surpasses that of asiatic acid.

In line with the *in vivo* observations, we observed that Hsp90 α , Hsp90 β , and PPAR γ expression was significantly increased in FFA-induced HepG2 cells (Figure 4D–G). However, silibinin normalized these aberrant alterations. To

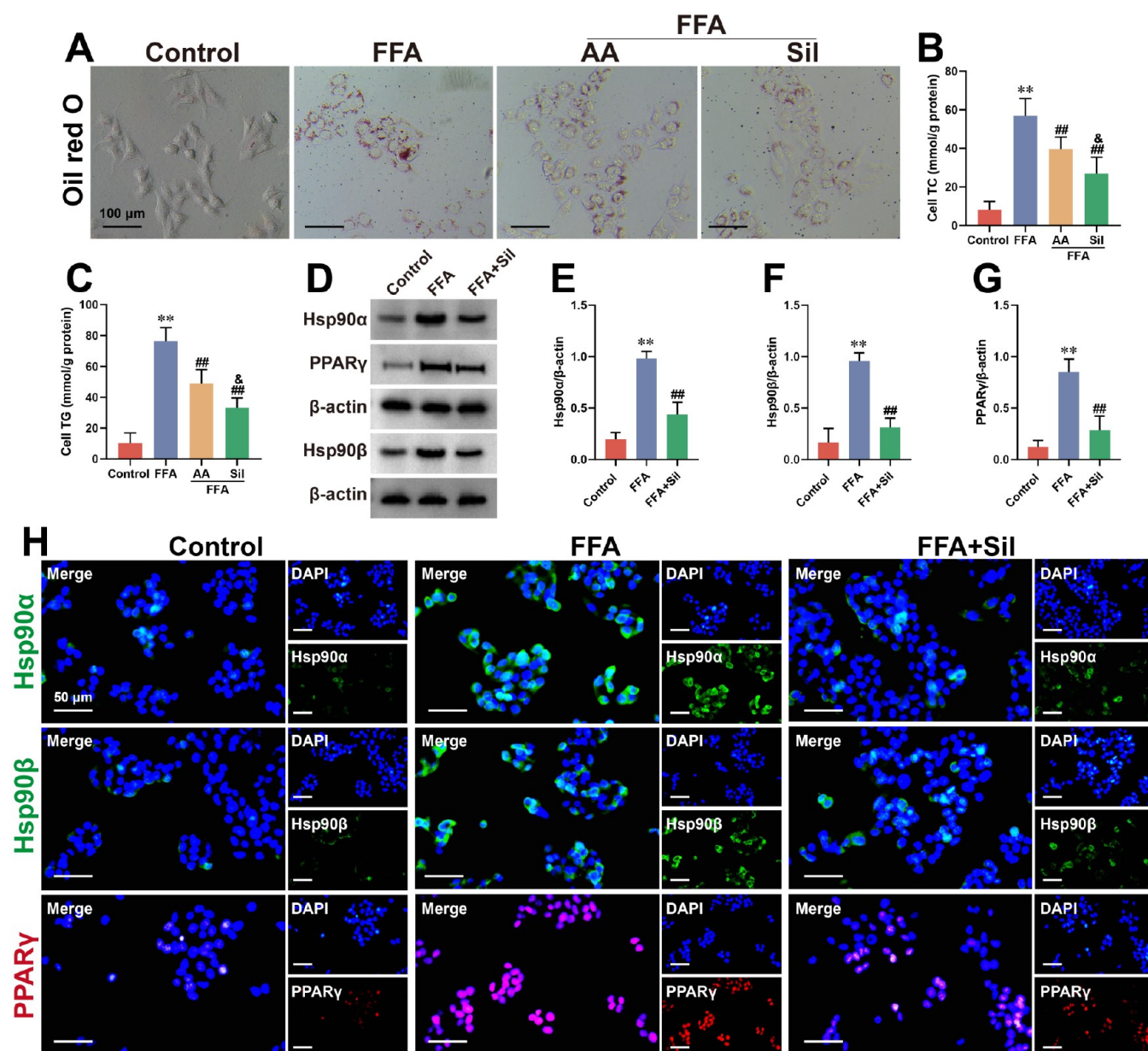


Figure 4. Silibinin alleviated lipotoxicity and suppressed the Hsp90/PPAR γ pathway in FFA-induced HepG2 cells. (A) Representative micrographs of Oil Red O of HepG2 cells. (B,C) The levels of TC and TG in HepG2 cells. (D) The expressions and (E–G) semiquantitative analysis of Hsp90 α , Hsp90 β , and PPAR γ . (H) Representative fluorescent photographs of Hsp90 α , Hsp90 β , and PPAR γ . Data are presented as the mean \pm SD ($n = 3$). ** $p < 0.01$ vs the control group, ### $p < 0.01$ vs the FFA group, and $p < 0.05$ vs the AA group. Sil, silibinin; AA, asiatic acid.

further determine the expression distribution of Hsp90 α , Hsp90 β , and PPAR γ , immunofluorescence analysis was performed. The fluorescence intensities of Hsp90 α and Hsp90 β were noticeably enhanced in the FFA group compared with the control group. Furthermore, PPAR γ nuclear translocation substantially increased in FFA-induced HepG2 cells, which was dramatically reversed after silibinin treatment (Figure 4H). Collectively, these findings suggest that silibinin protects hepatocytes from FFA-induced damage by inhibiting the Hsp90–PPAR γ pathway.

Next, to validate that the mitigatory effects of silibinin in FFA-induced HepG2 cells were achieved by inhibiting the Hsp90–PPAR γ pathway, Hsp90 was transiently overexpressed in HepG2 cells by cotransfecting Hsp90 α and Hsp90 β overexpression plasmids. In Hsp90-overexpressing cells, the

protein levels and fluorescence intensity of Hsp90 α , Hsp90 β , and PPAR γ increased (Figure 5A–E). Furthermore, lipid accumulation and TC and TG levels were increased. In addition, Hsp90 overexpression counteracted the regulatory effects of silibinin on the Hsp90/PPAR γ pathway as well as its ameliorative effects on lipotoxicity (Figure 5F–H). Collectively, our findings emphasize that silibinin protects against hepatic lipotoxicity by inhibiting the Hsp90/PPAR γ pathway.

3.4. Silibinin Ameliorated Gut Microbiota Dysbiosis in HFD-Induced NAFLD Mice. The gut microbiota comprises mucosal flora and luminal microbiota and adheres to the intestinal mucosal layer; it helps establish a multilayered gut microbial barrier. In this context, alpha diversity, an ecological measure that quantifies species richness and evenness within each sample, plays an essential role. As

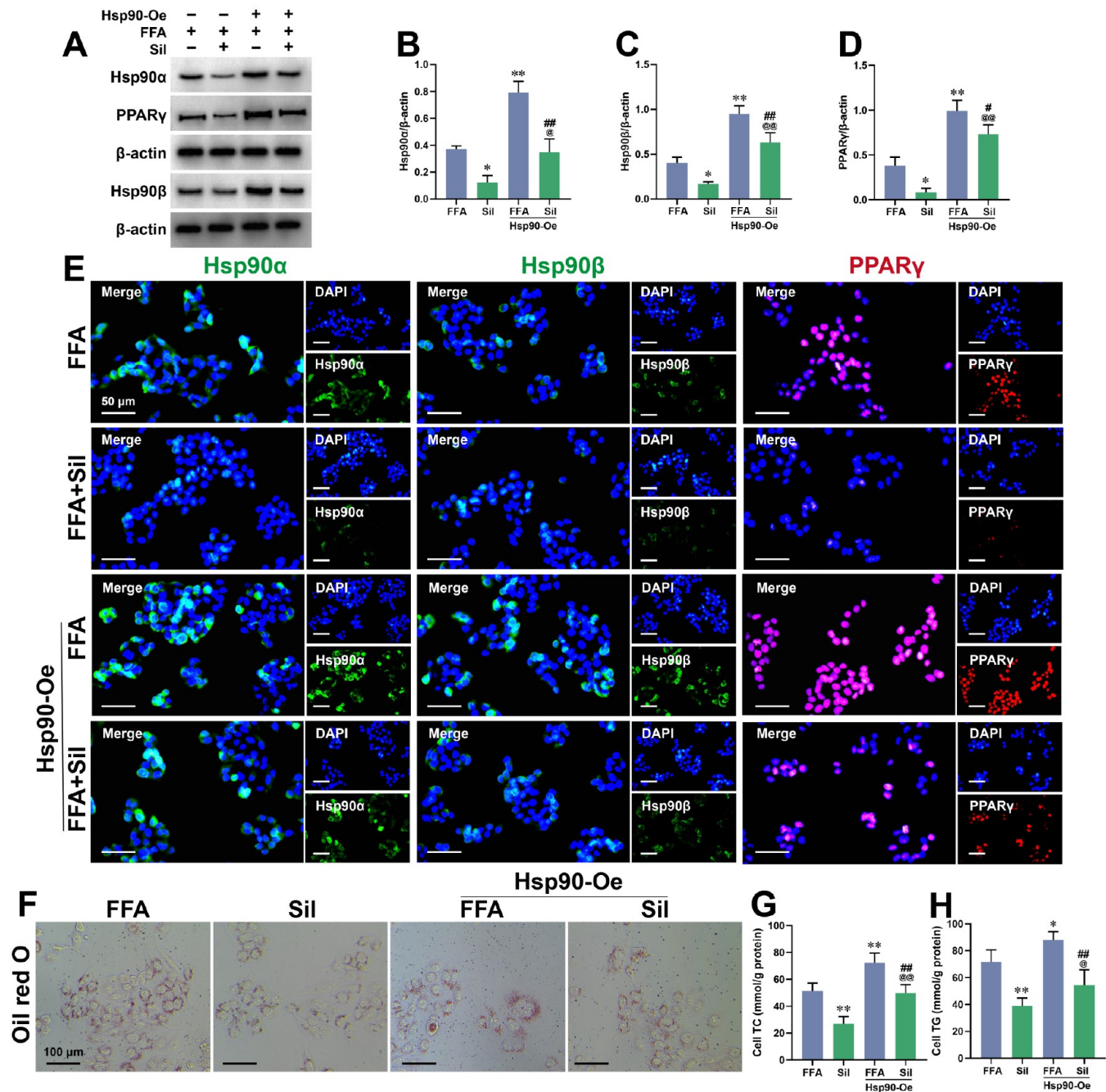


Figure 5. Silibinin exhibited hepatocyte protective efficacy by targeting the Hsp90/PPAR γ pathway in FFA-induced HepG2 cells. (A) The expressions and (B–D) semiquantitative analysis of Hsp90 α , Hsp90 β , and PPAR γ without or with Hsp90 overexpression (Hsp90-Oe). (E) Representative fluorescent photographs of Hsp90 α , Hsp90 β , and PPAR γ without or with Hsp90-Oe. (F) Representative micrographs of Oil Red O of HepG2 cells without or with Hsp90-Oe. (G,H) The levels of TC and TG in HepG2 cells without or with Hsp90-Oe. Data are presented as the mean \pm SD ($n = 3$). * $p < 0.05$ and ** $p < 0.01$ vs the FFA group, @ $p < 0.05$ and @@ $p < 0.01$ vs the Sil group, # $p < 0.05$, and ## $p < 0.01$ vs the FFA with Hsp90-Oe group. Sil, silibinin.

demonstrated in Figure 6A,B, alpha diversity was significantly lower in the HFD group compared with the NCD group, as indicated by the Sobs and Chao indexes. In contrast, the alpha diversity markedly increased in the silibinin group. Beta diversity, on the other hand, is a measure for characterizing the composition and differences between microbial communities. To assess the beta diversity of the groups, hierarchical clustering analysis (HCA) and principal component analysis (PCA) were performed. Figure 6C,D illustrates the HCA and PCA plots. Distinct clustering was observed between the NCD

and HFD groups; this suggests that HFD significantly affects the community structures of the gut microbiota. However, silibinin administration considerably altered the affected community structures, favoring a shift toward the NCD group. Figure 6E,F illustrates the relative abundance of the major bacteria at the phylum and genus levels. Variations in gut microbiota composition were observed among the groups. Figure 6G–P illustrates that the ratio of Firmicutes to Bacteroidota and the abundance of *Dubosiella*, *unclassified_f_Lachnospiraceae*, *norank_f_Lachnospiraceae*, *Bacteroides*,

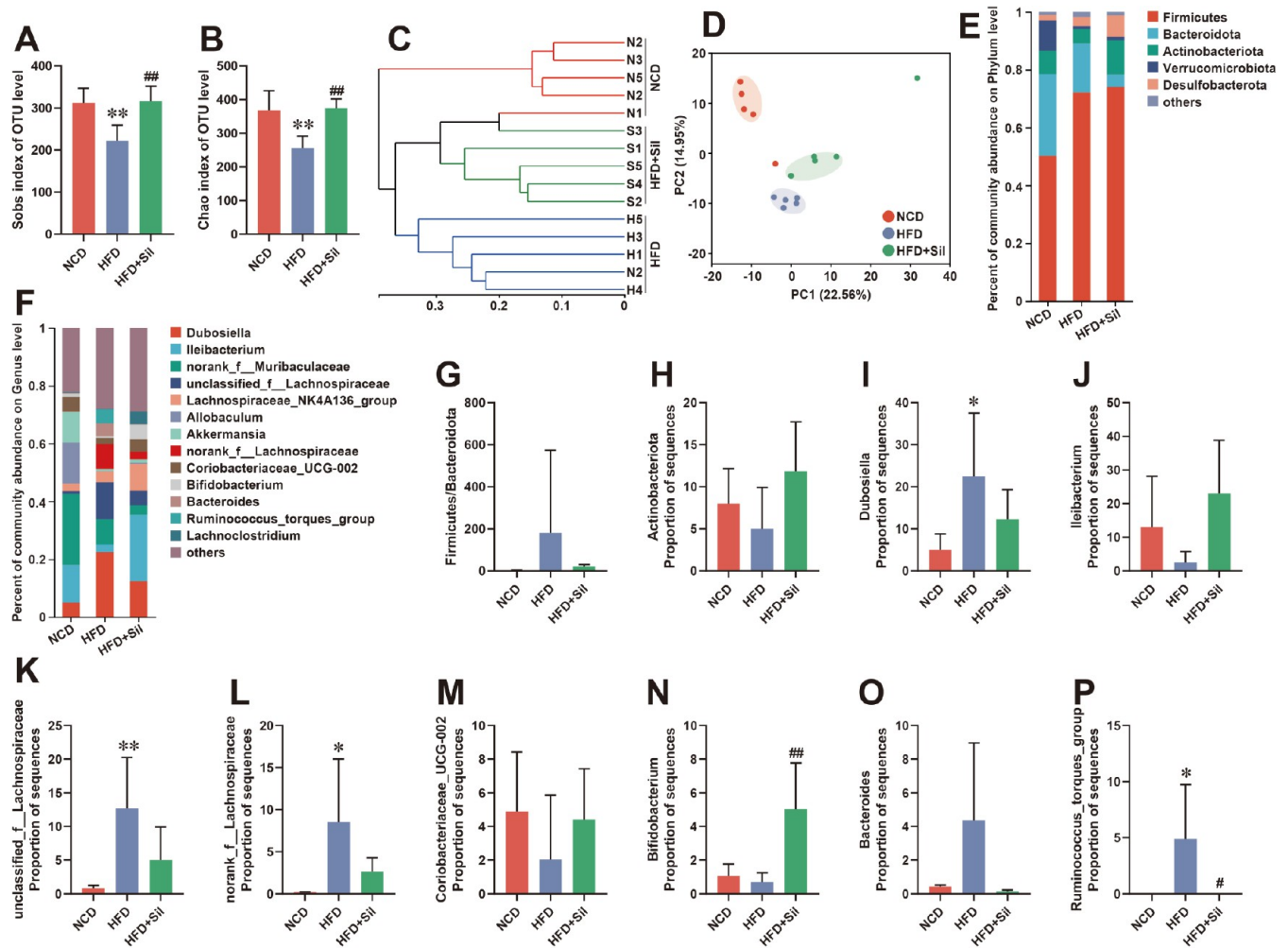


Figure 6. Silibinin normalized the general composition and abundance of the gut microbiota in HFD-fed mice. Alpha diversity of gut microbiota including Sobs index (A) and Chao index (B). Beta diversity of the gut microbiota as measured by HCA analysis (C) and PCA analysis (D). Relative abundance of species at the phylum level (E) and genus level (F) including (G–P) Firmicutes to Bacteroidota, Actinobacteriota, *Dubosiella*, *Ileibacterium*, *unclassified_f_Lachnospiraceae*, *norank_f_Lachnospiraceae*, *Coriobacteriaceae_UCG-002*, *Bifidobacterium*, *Bacteroides*, and *Ruminococcus_torques_group*. Data are presented as the mean \pm SD ($n = 5$). * $p < 0.05$ and ** $p < 0.01$ vs the NCD group and ## $p < 0.01$ vs the HFD group. Sil, silibinin.

and *Ruminococcus_torques_group* were increased in the HFD group compared with the NCD group. In contrast, the abundance of Actinobacteriota, *Ileibacterium*, *Coriobacteriaceae_UCG-002*, and *Bifidobacterium* was decreased in the HFD group. However, silibinin administration corrected these perturbed alterations. Overall, these findings suggest that silibinin can reinstate gut barrier function by modulating gut microbiota composition.

3.5. Silibinin Maintained Gut Barrier Function by Regulating the Hsp90/NLRP3 Pathway in HFD-Fed Mice. The activation of NLRP3, an Hsp90 client protein, induces inflammation, resulting in increased intestinal epithelial permeability and dysfunction.¹³ Furthermore, intestinal microbiota dysbiosis additionally activates NLRP3, perpetuating a relentless cycle of inflammatory responses, exacerbating the adverse implications of gut barrier function.¹⁴ In the present study, we investigated the effect of silibinin on the gut barrier by determining intestinal epithelial structure integrity. Figure 7A demonstrates that HFD intervention resulted in atrophy and shortening and fracturing of the colon villi; silibinin effectively attenuated these phenomena. More-

over, PAS staining revealed that goblet cells were significantly depleted, and mucus secretion was decreased in the HFD group; nevertheless, they were restored after silibinin treatment (Figure 7B). Mucins (e.g., MUC2), secreted by goblet cells, and water, form a mucus layer that attaches to the intestinal epithelium; this layer plays a vital role in maintaining gut function. Tight junction (TJ) proteins (e.g., ZO-1, occludin, claudin-1) maintain the integrity and selective permeability of intestinal epithelial cells. As demonstrated in Figure 7C–F, the protein levels of MUC2, ZO-1, and occludin were significantly decreased in the HFD group compared with the NCD group; however, silibinin administration effectively reversed these changes. Consistently, immunohistochemical analysis confirmed the low-staining intensity (brown) for MUC2, ZO-1, and occludin in the HFD group; silibinin treatment substantially restored the altered levels (Figure 7G–J). Taken together, these findings suggest that silibinin exerts a beneficial effect on HFD-induced gut barrier function dysfunction.

Next, we measured the levels of Hsp90 α , Hsp90 β , and NLRP3 inflammasome-related proteins (e.g., NLRP3, ASC,

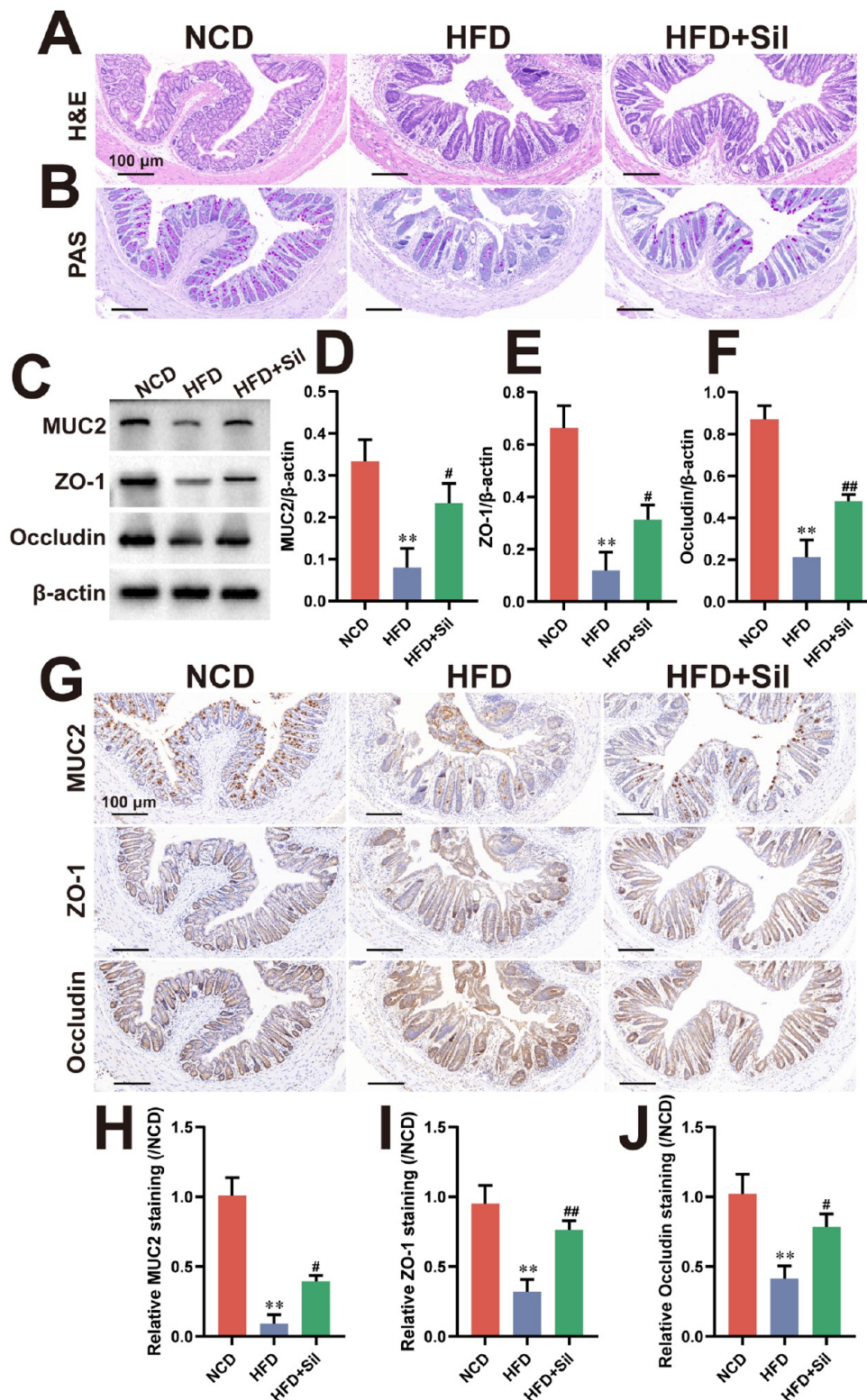


Figure 7. Silibinin ameliorated gut barrier function dysfunction in HFD-fed mice. Representative micrographs of H&E (A) and PAS (B) stainings. (C) Expression levels and (D–F) semiquantitative analysis of MUC2, ZO-1, and occludin. (G) Representative immunohistochemical images and (H–J) quantitative analysis of the staining intensity of MUC2, ZO-1, and occludin in colon sections. Data were denoted as the mean \pm SD ($n = 3$). ** $p < 0.01$ vs the NCD group and # $p < 0.05$ and ## $p < 0.01$ vs the HFD group. Sil, silibinin.

caspase-1). **Figure 8A–F** demonstrates that the protein levels of Hsp90 α , Hsp90 β , NLRP3, ASC, and caspase-1 were significantly increased in the HFD group compared with the NCD group; however, silibinin strikingly reversed these

alterations. Consistent with the above-mentioned findings, immunological analysis further substantiated the robust immunostaining intensity (brown/fluorescence) of Hsp90 α , Hsp90 β , NLRP3, ASC, and caspase-1 in the HFD group,

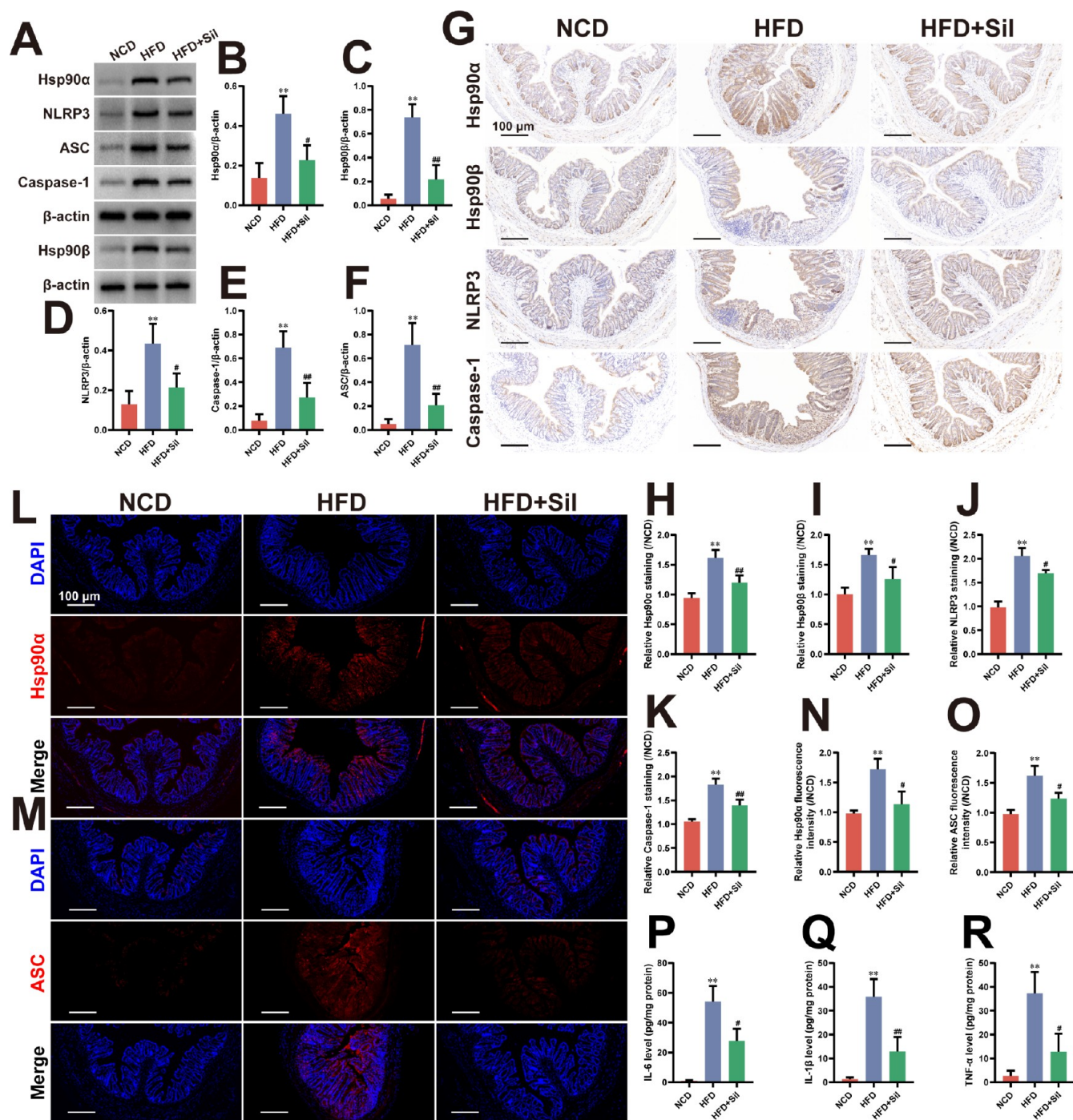


Figure 8. Silibinin blunted the Hsp90/NLRP3 pathway-mediated inflammation in HFD-fed mice. (A) Expression levels and (B–F) semiquantitative analysis of Hsp90 α , Hsp90 β , NLRP3, ASC, and caspase-1. (G) Representative immunohistochemical images and (H–K) quantitative analysis of the intensity of Hsp90 α , Hsp90 β , NLRP3, and caspase-1 in colon sections. (L–M) Representative fluorescent images and (N–O) quantitative analysis of the fluorescence intensity of Hsp90 α and ASC in colon sections. (P–R) colonic levels of IL-6, IL-1 β , and TNF- α . Data were denoted as the mean \pm SD ($n = 3$). ** $p < 0.01$ vs the NCD group and # $p < 0.05$ and ## $p < 0.01$ vs the HFD group. Sil, silibinin.

indicating the increased levels of these proteins (Figure 8G–O). However, silibinin notably mitigated the increased staining intensities of these proteins, corroborating the inhibitory effect of silibinin on the Hsp90–NLRP3 pathway in the gut. Importantly, Figure 8P–R illustrates a marked increase in IL-6, IL-1 β , and TNF- α levels in the colon of HFD-fed mice compared with that of NCD-fed mice; this indicates an NLRP3 inflammasome-induced inflammatory response in the colon. However, these changes were distinctly reversed after

silibinin treatment. Taken together, our findings suggest that the inhibition of the Hsp90/NLRP3 pathway may mediate the benefits of silibinin on HFD-induced gut barrier dysfunction.

4. DISCUSSION

Owing to its continuously growing incidence and severe adverse outcomes, NAFLD considerably affects the quality of life of patients. Accordingly, researchers have focused on identifying effective medications to combat NAFLD, and

herbal and/or natural compounds, such as asiatic acid, exhibit outstanding potential to target multiple aberrant pathways.^{31–33} Clinical studies on silibinin, a flavonoid with hepatoprotective properties, are ongoing to investigate its efficacy against NAFLD.³⁴ However, the limited understanding of its mechanisms of action and insufficient therapeutic evidence hamper its utilization for patients with NAFLD. Herein, we provided holistic preclinical evidence to support the use of silibinin against NAFLD, thereby shedding more light on latent mechanisms from the intrahepatic and extrahepatic perspectives. Silibinin effectively mitigated HFD-induced obesity, hepatic steatosis, lipid disorder, and liver damage and reduced FFA-evoked lipid accumulation by inhibiting Hsp90/PPAR γ -mediated hepatic lipotoxicity and Hsp90/NLRP3-mediated gut dysfunction and modulating intestinal microbiota. These remarkable results indicate that silibinin holds great promise as a candidate drug for treating NAFLD.

The overconsumption of an HFD has been progressively prevalent in modern society, which markedly contributes to NAFLD development.³⁰ Thus, to establish NAFLD animal models that can well mirror symptoms observed in patients with NAFLD, an HFD is routinely fed to the animals.^{27,28,30} Oleic and palmitic acids, the two main fatty acids driving the TG buildup, are a hallmark of NAFLD.³⁵ The exogenous supplementation of these acids can simulate NAFLD pathology in hepatocytes *in vitro*.³⁰ Herein, HFD-fed mice and FFA-stimulated HepG2 cells were selected to investigate the effects of silibinin on NAFLD. Consistent with previous results, a 16-week HFD-feeding regimen in the present study induced severe obesity, hepatic steatosis, lipid abnormality, and liver injury. Additionally, the FFA-stimulated HepG2 cells exhibited noticeable lipid accumulation that was accompanied by increased intracellular TC and TG levels. Moreover, these aberrant alterations were almost entirely mitigated by silibinin, indicating its robust efficacy against NAFLD.

The multiple-hit hypothesis showed that hepatic steatosis initiated the subsequent cascade of intrahepatic detrimental events.⁵ Hsp90, a pivotal molecular chaperone protein, exhibits indispensable functions in lipid and glucose metabolism regulation, especially in hepatocytes.^{7,10} Clinical studies have revealed increased Hsp90 α and Hsp90 β levels in the serum of patients with NAFLD, which were positively correlated with the severity of hepatic steatosis.^{36,37} Furthermore, the Hsp90 N-terminal inhibitor 17-AAG enhances hepatic albumin accumulation in mice, thereby inhibiting NAFLD progression.³⁸

PPAR γ plays a dual role in the livers to facilitate the uptake and synthesis of both the fatty acids and prevent their catabolism, leading to lipid accumulation. Additionally, PPAR γ promotes adipogenesis and regulates adipocyte apoptosis and inflammation, indicating its potential in treating NAFLD and NASH.³⁹ PPAR γ antagonists help effectively manage obesity and diabetes by preventing fat accumulation in adipocytes and enhancing insulin sensitivity.⁴⁰ Compounds such as tanshinone IIA, ginsenoside Rg3, maslinic acid, and licochalcone A protect animals from NAFLD by repressing PPAR γ activity, which is evidenced by improved cell differentiation, reduced 3T3-L1 adipocyte lipogenesis, and decreased hepatic steatosis in HFD-induced mice.⁴¹ An interaction between Hsp90 and PPAR γ has helped elucidate the role of Hsp90 in enhancing PPAR γ stability and functionality, thereby highlighting its regulatory effect on lipid metabolism.^{10,11} Compared with conventional

N-terminal inhibitors, the C-terminal Hsp90 inhibitor silibinin exhibits a superior safety profile.^{20,41} Herein, the liver transcriptome analysis showed that silibinin exerted negative regulatory effects on the Hsp90/PPAR γ pathway. Increased *Hsp90aa1*, *Hsp90ab1*, and *Ppar γ* mRNA levels and Hsp90 α , Hsp90 β , and PPAR γ protein levels were observed in HFD- and FFA-induced NAFLD models, which indicated Hsp90/PPAR γ pathway activation in NAFLD. However, silibinin intervention effectively reversed the aforementioned increased levels. Moreover, Hsp90 overexpression in HepG2 cells further confirmed that the favorable effects of silibinin on hepatic steatosis were Hsp90/PPAR γ -pathway-dependent.

In NAFLD pathogenesis, the gut is the principal hub for extrahepatic detrimental factors. Additionally, perturbations of the gut barrier function, encompassing structural alterations in the intestinal epithelial cell layer, mucosal mucus layer impairment, and gut microbiota dysbiosis, are evident in patients with NAFLD and HFD-fed experimental animals.⁴² An intact gut barrier comprises the epithelium consisting of absorptive enterocytes, mucus-producing goblet cells, anti-microbial peptide-producing Paneth cells, and hormone-producing enteroendocrine cells.²⁹ Moreover, the disruption of the physical barrier increases the permeability of the intestine and enables the translocation of detrimental substances in food and undesirable bacterial metabolites into the systemic circulation.²⁹ TJ proteins and mucins are necessary for epithelial integrity and selective paracellular permeability. Despite the inherent limited bioavailability of some natural products, they have exhibited efficacy in combating NAFLD when administered orally.⁴² These favorable outcomes are because of the unabsorbed fraction of these compounds that exert therapeutic effects on the liver via the complex gut–liver axis.^{30,42} For instance, the effect of arjunolic acid on NAFLD was partly mediated by its unabsorbed fraction, which restored the structure of intestinal epithelial cells and improved the gut barrier function.³⁰ Furthermore, a Ganoderma meroterpene derivative without a direct effect on hepatocytes ameliorated the intrahepatic inflammatory response by upregulating claudin-1 and ZO-1 expression and modulating gut microbiota compositions.⁴³

Similarly, herein, the oral administration of silibinin showed the noticeable alleviation of HFD-induced structural impairment in epithelial and goblet cells and the downregulation of MUC2, ZO-1, and occludin expression, which indicated the reparative effects of silibinin on epithelial integrity. Previous studies have shown notable differences in gut microbiota compositions between patients with NAFLD and normal individuals. Consequently, multiple studies have been performed to investigate the therapeutic efficacy of gut microbiota modulation for NAFLD, such as gut microbiota transplantation.⁴⁴ Herein, we found that the oral administration of silibinin reversed HFD-induced gut microbiota dysbiosis, which was evidenced by the recovered microbial diversity and community composition. Compared with the HFD-fed mice, remarkable changes in the relative abundance of specific bacteria in the silibinin-treated mice were observed, which were characterized by increased abundances of Actinobacteriota, *Ileibacterium*, *Coriobacteriaceae_UCG-002*, and *Bifidobacterium* and decreased abundances of the Firmicutes-to-Bacteroidota ratio, *Dubosiella*, *unclassified_f_Lachnospiraceae*, *norank_f_Lachnospiraceae*, *Bacteroides*, and *p. Actinobacteriota* produces SCFAs that permeate the impaired intestinal epithelium and affect various physiological and

pathological processes associated with NAFLD.⁴⁵ Additionally, alterations in *Bifidobacterium* and *Bacteroides* abundances in patients with NAFLD have been reported.⁴⁶ *Bifidobacterium*, a recognized probiotic, modifies the gut microbiota, improves the gut barrier function, and decreases intestinal inflammation.⁴⁷ Moreover, *Bifidobacterium* and metabolites produced by specific *Bacteroides* species affect lipid metabolism, insulin resistance, and liver inflammation, all of which are crucial for NAFLD development.^{46,47} Patients with NAFLD often show a higher ratio of Firmicutes/Bacteroidota, which was attributed to increased energy extraction from the diet, compromised gut barrier functions, and improved intestinal permeability.^{48,49} Herein, we observed a normalization of the relative abundances of these bacteria in the silibinin-treated group. Overall, the results indicate that silibinin can effectively ameliorate HFD-induced gut barrier injury and gut dysbiosis.

Intestinal inflammation directly affects intestinal epithelial cells, resulting in cell damage, apoptosis, altered metabolic activity, and TJ breakdown, thereby compromising the gut barrier function.^{13,14} The presence of intestinal mucosal inflammation contributed to the impaired gut barrier function in patients with NAFLD and animal models.⁵⁰ The NLRP3 inflammasome is pivotal in activating intestinal immune cells and inducing intestinal inflammation/injuries and is often activated by prolonged HFD induction, harmful bacteria, and toxins.^{48,51} Once subjected to an adverse stimulus for an extended period, the activated NLRP3 inflammasome in the intestine initially interacts with ASC, which promotes procaspase-1 recruitment to assemble the NLRP3 inflammasome, eventually activating caspase-1 and initiating a cascade of inflammatory responses in the intestine.⁴⁸ NLRP3 is highly expressed in the colon of HFD-fed rats, and *Astragalus mongholicus* polysaccharides alleviate intestinal inflammation and NAFLD by lowering NLRP3 levels in the colon.⁴⁸ NLRP3 is a client protein of Hsp90, and the stability of the Hsp90/NLRP3 complex is crucial for NLRP3 to form the inflammasome.⁵² Hsp90 inhibition may mediate NLRP3 inflammasome inactivation and mitigate Parkinson's disease by exerting anti-inflammatory effects.⁵³ Silibinin, a specific inhibitor of Hsp90, can exert reparative effects on inflammation-induced intestinal epithelial damage by blocking the Hsp90/NLRP3 pathway. Herein, markedly increased Hsp90 α , Hsp90 β , NLRP3, ASC, caspase-1, IL-6, IL-1 β , and TNF- α levels in the colons of NAFLD mice indicated the occurrence of Hsp90/NLRP3 pathway-mediated intestinal inflammation. Silibinin intervention remarkably attenuated these alterations, suggesting that the drug effectively mitigated the degradation of the gut inflammation-mediated barrier by suppressing the Hsp90/NLRP3 pathway.

5. CONCLUSIONS

In conclusion, the present study showed that silibinin exerted multiple therapeutic effects on NAFLD, including improvements in adiposity, hepatic steatosis, lipid disorders, liver injury, gut barrier disruption, and gut microbiota dysbiosis. These favorable effects were closely related to the inhibition of Hsp90/PPAR γ -mediated hepatic lipotoxicity and depression of Hsp90/NLRP3-evoked gut inflammation. The present results highlight silibinin as a multifaceted therapeutic agent for NAFLD. We are the first to elucidate its potential mechanisms of action from multiple-hit perspectives (i.e., intrahepatic and extrahepatic).

AUTHOR INFORMATION

Corresponding Author

Tingming Fu – School of Pharmacy, Nanjing University of Chinese Medicine, Nanjing 210023, China; orcid.org/0000-0003-4196-6787; Email: futm@njucm.edu.cn

Authors

Baofei Yan – School of Pharmacy, Nanjing University of Chinese Medicine, Nanjing 210023, China; Jiangsu Engineering, Research Center for Evaluation and Transformation of Classic TCM Prescriptions, Jiangsu Health Vocational College, Nanjing 211800, China
Xian Zheng – Department of Pharmacy, Affiliated Kunshan Hospital of Jiangsu University, Kunshan 215399, China
Xi Chen – Institute of Medical technology, Jiangsu College of Nursing, Huaian 223003, China
Huohui Hao – Department of Pharmacology, Jiangsu College of Nursing, Huaian 223003, China
Shen Shen – School of Pharmacy, Nanjing University of Chinese Medicine, Nanjing 210023, China
Jingwen Yang – School of Pharmacy, Nanjing University of Chinese Medicine, Nanjing 210023, China
Siting Wang – School of Pharmacy, Nanjing University of Chinese Medicine, Nanjing 210023, China
Yuping Sun – School of Pharmacy, Nanjing University of Chinese Medicine, Nanjing 210023, China
Jiaqi Xian – School of Pharmacy, Nanjing University of Chinese Medicine, Nanjing 210023, China
Zhitao Shao – School of Pharmacy, Nanjing University of Chinese Medicine, Nanjing 210023, China

Complete contact information is available at:
<https://pubs.acs.org/10.1021/acsptsci.4c00185>

Author Contributions

[#]B.Y. and X.Z. contributed equally to this work. T.F. contributed to conceptualization; J.Y. and X.C. contributed to methodology; B.Y., X.Z., and Z.S. contributed to formal analysis; Z.S. and J.X. contributed to software; S.W. and Y.S. contributed to investigation; B.Y., X.Z., H.H., and X.C. contributed to writing – original draft; T.F. and X.Z. contributed to writing – review and editing; T.F., X.Z., and B.Y. contributed to funding acquisition.

Funding

The work was financially supported by the National Natural Science Foundation of China (82304807), the Primary Research and Development Plan of Jiangsu Province, China (BE2019721), the Science and Technology Innovation Fund of the Dantu District (GY2021001), the Suzhou Science and Technology Bureau Development Plan (SKYD2023171), the Scientific Research Project of Jiangsu Health Commission (Z2022078), the Kunshan Key Research and Development Plan (KS2203), the Major Project of School-Level Research at Jiangsu Health Vocational College (JKA202203), and the Huaian City Science and Technology Plan Project (HAB202135).

Notes

The authors declare no competing financial interest.

ACKNOWLEDGMENTS

The authors are grateful to Yue-Tao He (Zhengsheng Biotechnology Co. Ltd.) for kindly providing high-quality reagents.

ABBREVIATIONS

NAFLD, nonalcoholic fatty liver disease; NAFL, nonalcoholic fatty liver; NASH, nonalcoholic steatohepatitis; CVD, cardiovascular disease; PPAR γ , peroxisome proliferator-activated receptor- γ ; TG, triglyceride; Hsp90, heat shock protein 90; NLRP3, NOD-like receptor pyrin domain-containing 3; *S. marianum*, *Silybum marianum*; HFD, high-fat diet; SCFAs, short-chain fatty acids; FFA, free fatty acid; Sil, silibinin; H&E, hematoxylin and eosin stain; PAS, periodic acid-schiff; IL-6, interleukin-6; IL-1 β , interleukin-1 β ; TNF- α , tumor necrosis factor- α ; TC, total cholesterol; LDL-c, low-density lipoprotein cholesterol; HDL-c, high-density lipoprotein cholesterol; ALT, alanine aminotransferase; AST, aspartate aminotransferase; DMEM, Dulbecco's modified Eagle medium; FBS, fetal bovine serum; BSA, bovine serum albumin; ASC, apoptosis-associated speck-like protein containing a CARD; MUC2, mucin 2; ZO-1, zonula occludens-1; NCD, normal chow diet; RT-PCR, real-time polymerase chain reaction; SD, standard deviation; DEGs, differentially expressed genes; HCA, hierarchical clustering analysis; PCA, principal component analysis; TJ, tight junction

REFERENCES

- Younossi, Z.; Anstee, Q. M.; Marietti, M.; Hardy, T.; Henry, L.; Eslam, M.; George, J.; Bugianesi, E. Global burden of NAFLD and NASH: trends, predictions, risk factors and prevention. *Nat. Rev. Gastroenterol. Hepatol.* **2018**, *15* (1), 11–20.
- Friedman, S. L.; Neuschwander-Tetri, B. A.; Rinella, M.; Sanyal, A. J. Mechanisms of NAFLD development and therapeutic strategies. *Nat. Med.* **2018**, *24* (7), 908–922.
- Targher, G.; Byrne, C. D.; Tilg, H. NAFLD and increased risk of cardiovascular disease: clinical associations, pathophysiological mechanisms and pharmacological implications. *Gut* **2020**, *69* (9), 1691–1705.
- Anania, C.; Perla, F. M.; Olivero, F.; Pacifico, L.; Chiesa, C. Mediterranean diet and nonalcoholic fatty liver disease. *World J. Gastroenterol.* **2018**, *24* (19), 2083–2094.
- Buzzetti, E.; Pinzani, M.; Tsochatzis, E. A. The multiple-hit pathogenesis of non-alcoholic fatty liver disease (NAFLD). *Metabolism* **2016**, *65* (8), 1038–1048.
- Liu, K.; Qiu, D.; Liang, X.; Huang, Y.; Wang, Y.; Jia, X.; Li, K.; Zhao, J.; Du, C.; Qiu, X.; Cui, J.; Xiao, Z.; Qin, Y.; Zhang, Q. Lipotoxicity-induced STING1 activation stimulates MTORC1 and restricts hepatic lipophagy. *Autophagy* **2022**, *18* (4), 860–876.
- Guilherme, A.; Virbasius, J. V.; Puri, V.; Czech, M. P. Adipocyte dysfunctions linking obesity to insulin resistance and type 2 diabetes. *Nat. Rev. Mol. Cell Biol.* **2008**, *9* (5), 367–377.
- Kurano, M.; Ikeda, H.; Iso, O. N.; Hara, M.; Tsukamoto, K.; Yatomi, Y. Regulation of the metabolism of apolipoprotein M and sphingosine 1-phosphate by hepatic PPAR γ activity. *Biochem. J.* **2018**, *475* (12), 2009–2024.
- Li, L.; Fu, J.; Liu, D.; Sun, J.; Hou, Y.; Chen, C.; Shao, J.; Wang, L.; Wang, X.; Zhao, R.; Wang, H.; Andersen, M. E.; Zhang, Q.; Xu, Y.; Pi, J. Hepatocyte-specific Nrf2 deficiency mitigates high-fat diet-induced hepatic steatosis: Involvement of reduced PPAR γ expression. *Redox Biol.* **2020**, *30*, 101412.
- Wheeler, M. C.; Gekakis, N. Hsp90 modulates PPAR γ activity in a mouse model of nonalcoholic fatty liver disease. *J. Lipid Res.* **2014**, *55* (8), 1702–1710.
- Nguyen, M. T.; Csermely, P.; Šti, C. Hsp90 chaperones PPAR γ and regulates differentiation and survival of 3T3-L1 adipocytes. *Cell Death Differ.* **2013**, *20* (12), 1654–1663.
- Aron-Wisniewsky, J.; Vigliotti, C.; Witjes, J.; Le, P.; Holleboom, A. G.; Verheij, J.; Nieuwdorp, M.; Clément, K. Gut microbiota and human NAFLD: Disentangling microbial signatures from metabolic disorders. *Nat. Rev. Gastroenterol. Hepatol.* **2020**, *17* (5), 279–297.
- Ferrucci, L.; Fabbri, E. Inflammageing: chronic inflammation in ageing, cardiovascular disease, and frailty. *Nat. Rev. Cardiol.* **2018**, *15* (9), 505–522.
- Canfora, E. E.; Meex, R. C. R.; Venema, K.; Blaak, E. E. Gut microbial metabolites in obesity, NAFLD and T2DM. *Nat. Rev. Endocrinol.* **2019**, *15* (5), 261–273.
- Nizami, S.; Arunasalam, K.; Green, J.; Cook, J.; Lawrence, C. B.; Zarganes-Tzitzikas, T.; Davis, J. B.; Di Daniel, E.; Brough, D. Inhibition of the NLRP3 inflammasome by HSP90 inhibitors. *Immunology* **2021**, *162* (1), 84–91.
- Xu, G.; Fu, S.; Zhan, X.; Wang, Z.; Zhang, P.; Shi, W.; Qin, N.; Chen, Y.; Wang, C.; Niu, M.; Guo, Y.; Wang, J.; Bai, Z.; Xiao, X. Echinatin effectively protects against NLRP3 inflammasome-driven diseases by targeting HSP90. *JCI Insight* **2021**, *6* (2), No. e134601.
- Abenavoli, L.; Izzo, A. A.; Milić, N.; Cicala, C.; Santini, A.; Capasso, R. Milk thistle (*Silybum marianum*): A concise overview on its chemistry, pharmacological, and nutraceutical uses in liver diseases. *Phytother. Res.* **2018**, *32* (11), 2202–2213.
- Wadhwa, K.; Pahwa, R.; Kumar, M.; Kumar, S.; Sharma, P. C.; Singh, G.; Verma, R.; Mittal, V.; Singh, I.; Kaushik, D.; Jeandet, P. Mechanistic insights into the pharmacological significance of silymarin. *Molecules* **2022**, *27* (16), 5327.
- Polachi, N.; Bai, G.; Li, T.; Chu, Y.; Wang, X.; Li, S.; Gu, N.; Wu, J.; Li, W.; Zhang, Y.; Zhou, S.; Sun, H.; Liu, C. Modulatory effects of silibinin in various cell signaling pathways against liver disorders and cancer-A comprehensive review. *Eur. J. Med. Chem.* **2016**, *123*, 577–595.
- Riebold, M.; Kozany, C.; Freiburger, L.; Sattler, M.; Buchfelder, M.; Hausch, F.; Stalla, G. K.; Paez-Pereda, M. A C-terminal HSP90 inhibitor restores glucocorticoid sensitivity and relieves a mouse allograft model of Cushing disease. *Nat. Med.* **2015**, *21* (3), 276–280.
- Suguro, R.; Pang, X. C.; Yuan, Z. W.; Chen, S. Y.; Zhu, Y. Z.; Xie, Y. Combinational application of silybin and tangeretin attenuates the progression of non-alcoholic steatohepatitis (NASH) in mice via modulating lipid metabolism. *Pharmacol. Res.* **2020**, *151*, 104519.
- Li, X.; Wang, Y.; Xing, Y.; Xing, R.; Liu, Y.; Xu, Y. Changes of gut microbiota during silybin-mediated treatment of high-fat diet-induced non-alcoholic fatty liver disease in mice. *Hepatol. Res.* **2020**, *50* (1), 5–14.
- Zheng, R.; Ma, J.; Wang, D.; Dong, W.; Wang, S.; Liu, T.; Xie, R.; Liu, L.; Wang, B.; Cao, H. Chemopreventive effects of silibinin on colitis-associated tumorigenesis by inhibiting IL-6/STAT3 signaling pathway. *Mediators Inflammation* **2018**, *2018*, 1562010.
- Ma, X.; Xia, K.; Xie, J.; Yan, B.; Han, X.; Li, S.; Wang, Y.; Fu, T. Treatment of Idiopathic Pulmonary Fibrosis by Inhaled Silybin Dry Powder Prepared via the Nanosuspension Spray Drying Technology. *ACS Pharmacol. Transl. Sci.* **2023**, *6* (6), 878–891.
- Sun, R.; Xu, D.; Wei, Q.; Zhang, B.; Aa, J.; Wang, G.; Xie, Y. Silybin ameliorates hepatic lipid accumulation and modulates global metabolism in an NAFLD mouse model. *Biomed. Pharmacother.* **2020**, *123*, 109721.
- Yan, B. F.; Pan, L. F.; Quan, Y. F.; Sha, Q.; Zhang, J. Z.; Zhang, Y. F.; Zhou, L. B.; Qian, X. L.; Gu, X. M.; Li, F. T.; Wang, T.; Liu, J.; Zheng, X. Huangqin decoction alleviates lipid metabolism disorders and insulin resistance in nonalcoholic fatty liver disease by triggering Sirt1/NF- κ B pathway. *World J. Gastroenterol.* **2023**, *29* (31), 4744–4762.
- Yan, B. F.; Zheng, X.; Wang, Y.; Yang, J. W.; Zhu, X. Y.; Qiu, M. M.; Xia, K. X.; Wang, Y. A.; Li, M.; Li, S. P.; Ma, X. N.; Xie, J. J.; Li, F. T.; Fu, T. M.; Li, W. Liposome-based silibinin for mitigating nonalcoholic fatty liver disease: dual effects via parenteral and intestinal routes. *ACS Pharmacol. Transl. Sci.* **2023**, *6* (12), 1909–1923.
- Yan, B. F.; Wang, Y.; Wang, W. B.; Ding, X. J.; Wei, B.; Liu, S. J.; Fu, T. M.; Chen, L.; Zhang, J. Z.; Liu, J.; Zheng, X. Huangqin decoction mitigates hepatic inflammation in high-fat diet-challenged rats by inhibiting TLR4/NF- κ B/NLRP3 pathway. *J. Ethnopharmacol.* **2023**, *303*, 115999.

- (29) Yan, B. F.; Chen, X.; Chen, Y. F.; Liu, S. J.; Xu, C. X.; Chen, L.; Wang, W. B.; Wen, T. T.; Zheng, X.; Liu, J. Aqueous extract of *Paeoniae Radix Alba* (*Paeonia lactiflora* Pall.) ameliorates DSS-induced colitis in mice by tuning the intestinal physical barrier, immune responses, and microbiota. *J. Ethnopharmacol.* **2022**, *294*, 115365.
- (30) Zheng, X.; Zhang, X. G.; Liu, Y.; Zhu, L. P.; Liang, X. S.; Jiang, H.; Shi, G. F.; Zhao, Y. Y.; Zhao, Z. W.; Teng, Y.; Pan, K.; Zhang, J.; Yin, Z. Q. Arjunolic acid from *Cyclocarya paliurus* ameliorates nonalcoholic fatty liver disease in mice via activating Sirt1/AMPK, triggering autophagy and improving gut barrier function. *J. Funct. Foods* **2021**, *86*, 104686.
- (31) Wang, D.; Lao, L.; Pang, X.; Qiao, Q.; Pang, L.; Feng, Z.; Bai, F.; Sun, X.; Lin, X.; Wei, J. Asiatic acid from *Potentilla chinensis* alleviates non-alcoholic fatty liver by regulating endoplasmic reticulum stress and lipid metabolism. *Int. Immunopharmacol.* **2018**, *65*, 256–267.
- (32) Niu, K.; Bai, P.; Yang, B.; Feng, X.; Qiu, F. Asiatic acid alleviates metabolism disorders in ob/ob mice: mechanistic insights. *Food Funct.* **2022**, *13* (13), 6934–6946.
- (33) Sharma, H.; Kumar, P.; Deshmukh, R. R.; Bishayee, A.; Kumar, S. Pentacyclic triterpenes: New tools to fight metabolic syndrome. *Phytomedicine* **2018**, *50*, 166–177.
- (34) Ren, L.; Ma, X. L.; Wang, H. L.; Li, R.; Cui, J. J.; Yan, P. J.; Wang, Y. N.; Yu, X. Y.; Du, P.; Yu, H. Y.; et al. Prebiotic-like cyclodextrin assisted silybin on NAFLD through restoring liver and gut homeostasis. *J. Controlled Release* **2022**, *348*, 825–840.
- (35) Araya, J.; Rodrigo, R.; Videla, L. A.; Thielemann, L.; Orellana, M.; Pettinelli, P.; Poniachik, J. Increase in long-chain polyunsaturated fatty acid n-6/n-3 ratio in relation to hepatic steatosis in patients with non-alcoholic fatty liver disease. *Clin. Sci.* **2004**, *106* (6), 635–643.
- (36) Xie, Y.; Chen, L.; Xu, Z.; Li, C.; Ni, Y.; Hou, M.; Chen, L.; Chang, H.; Yang, Y.; Wang, H.; He, R.; Chen, R.; Qian, L.; Luo, Y.; Zhang, Y.; Li, N.; Zhu, Y.; Ji, M.; Liu, Y. Predictive modeling of MAFLD based on Hsp90 α and the therapeutic application of teprenone in a diet-induced mouse model. *Front. Endocrinol.* **2021**, *12*, 743202.
- (37) Zheng, Z. G.; Zhang, X.; Liu, X. X.; Jin, X. X.; Dai, L.; Cheng, H. M.; Jing, D.; Thu, P. M.; Zhang, M.; Li, H. Y.; Zhu, J.; Liu, C.; Xue, B.; Li, Y.; Chen, L. G.; Peng, C.; Zhu, W. L.; Wang, L.; Liu, J. L.; Li, H. J.; Li, P.; Xu, X. J. Inhibition of HSP90 β improves lipid disorders by promoting mature SREBPs degradation via the ubiquitin-proteasome system. *Theranostics* **2019**, *9* (20), 5769–5783.
- (38) Ma, B.; Ju, A.; Zhang, S.; An, Q.; Xu, S.; Liu, J.; Yu, L.; Fu, Y.; Luo, Y. Albumosomes formed by cytoplasmic pre-folding albumin maintain mitochondrial homeostasis and inhibit nonalcoholic fatty liver disease. *Signal Transduction Targeted Ther.* **2023**, *8* (1), 229.
- (39) Lee, S. M.; Muratalla, J.; Sierra-Cruz, M.; Cordoba-Chacon, J. Role of hepatic peroxisome proliferator-activated receptor γ in non-alcoholic fatty liver disease. *J. Endocrinol.* **2023**, *257* (1), No. e220155.
- (40) Takada, I.; Makishima, M. Peroxisome proliferator-activated receptor agonists and antagonists: A patent review (2014-present). *Expert Opin. Ther. Pat.* **2020**, *30* (1), 1–13.
- (41) Jhaveri, K.; Ochiana, S. O.; Dunphy, M. P.; Gerecitano, J. F.; Corben, A. D.; Peter, R. I.; Janjigian, Y. Y.; Gomes-DaGama, E. M.; Koren, J., 3rd; Modi, S.; Chiosis, G. Heat shock protein 90 inhibitors in the treatment of cancer: Current status and future directions. *Expert Opin. Invest. Drugs* **2014**, *23* (5), 611–628.
- (42) Zeng, S. L.; Li, S. Z.; Xiao, P. T.; Cai, Y. Y.; Chu, C.; Chen, B. Z.; Li, P.; Li, J.; Liu, E. H. Citrus polymethoxyflavones attenuate metabolic syndrome by regulating gut microbiome and amino acid metabolism. *Sci. Adv.* **2020**, *6* (1), No. eaax6208.
- (43) Qiao, S.; Bao, L.; Wang, K.; Sun, S.; Liao, M.; Liu, C.; Zhou, N.; Ma, K.; Zhang, Y.; Chen, Y.; Liu, S.; Liu, H. Activation of a specific gut bacteroides-folate-liver axis benefits for the alleviation of nonalcoholic hepatic steatosis. *Cell Rep.* **2020**, *32* (6), 108005.
- (44) Milosevic, I.; Vujovic, A.; Barac, A.; Djelic, M.; Korac, M.; Radovanovic Spurnic, A.; Gmizic, I.; Stevanovic, O.; Djordjevic, V.; Lekic, N.; Russo, E.; Amedei, A. Gut-liver axis, gut microbiota, and its modulation in the management of liver diseases: A review of the literature. *Int. J. Mol. Sci.* **2019**, *20* (2), 395.
- (45) Liu, G.; Gu, K.; Liu, X.; Jia, G.; Zhao, H.; Chen, X.; Wang, J. Dietary glutamate enhances intestinal immunity by modulating microbiota and Th17/Treg balance-related immune signaling in piglets after lipopolysaccharide challenge. *Food Res. Int.* **2023**, *166*, 112597.
- (46) Zhang, X.; Coker, O. O.; Chu, E. S.; Fu, K.; Lau, H. C. H.; Wang, Y. X.; Chan, A. W. H.; Wei, H.; Yang, X. Y.; Sung, J. J. Y.; Yu, J. Dietary cholesterol drives fatty liver-associated liver cancer by modulating gut microbiota and metabolites. *Gut* **2021**, *70* (4), 761–774.
- (47) Cheng, J.; Laitila, A.; Ouwehand, A. C. Bifidobacterium animalis subsp. lactis HN019 effects on gut health: A review. *Front. Nutr.* **2021**, *8*, 790561.
- (48) Zhong, M.; Yan, Y.; Yuan, H.; Rong, A.; Xu, G.; Cai, F.; Yang, Y.; Wang, Y.; Zhang, W. Astragalus mongholicus polysaccharides ameliorate hepatic lipid accumulation and inflammation as well as modulate gut microbiota in NAFLD rats. *Food Funct.* **2022**, *13* (13), 7287–7301.
- (49) Murphy, E. F.; Cotter, P. D.; Hogan, A.; O'Sullivan, O.; Joyce, A.; Fouhy, F.; Clarke, S. F.; Marques, T. M.; O'Toole, P. W.; Stanton, C.; Quigley, E. M. M.; Daly, C.; Ross, P. R.; O'Doherty, R. M.; Shanahan, F. Divergent metabolic outcomes arising from targeted manipulation of the gut microbiota in diet-induced obesity. *Gut* **2013**, *62* (2), 220–226.
- (50) Mohamad nor, M. H.; Ayob, N.; Mokhtar, N. M.; Tan, G. C.; Wong, Z.; Shafiee, N. H.; Wong, Y. P.; Mustangin, M.; Nawawi, K. N. M. The effect of probiotics (MCP®) BCMC® Strains) on hepatic steatosis, small intestinal mucosal immune function, and intestinal barrier in patients with non-alcoholic fatty liver disease. *Nutrients* **2021**, *13* (9), 3192.
- (51) Nie, Y.; Liu, Q.; Zhang, W.; Wan, Y.; Huang, C.; Zhu, X. Ursolic acid reverses liver fibrosis by inhibiting NOX4/NLRP3 inflammasome pathways and bacterial dysbiosis. *Gut Microbes* **2021**, *13* (1), 1972746.
- (52) Shaaban, A. A.; Abdelhamid, A. M.; Shaker, M. E.; Cavalu, S.; Maghiar, A. M.; Alsayegh, A. A.; Babalghith, A. O.; El-Ahwany, E.; Amin, N. A.; Mohammed, O. A.; Eissa, H.; Gaafar, A.; Batiha, G. E.; Saber, S. Combining the HSP90 inhibitor TAS-116 with metformin effectively degrades the NLRP3 and attenuates inflammasome activation in rats: A new management paradigm for ulcerative colitis. *Biomed. Pharmacother.* **2022**, *153*, 113247.
- (53) Yan, Y. Q.; Zheng, R.; Liu, Y.; Ruan, Y.; Lin, Z. H.; Xue, N. J.; Chen, Y.; Zhang, B. R.; Pu, J. L. Parkin regulates microglial NLRP3 and represses neurodegeneration in Parkinson's disease. *Aging Cell* **2023**, *22* (6), No. e13834.